

Available at [www.sciencedirect.com](http://www.sciencedirect.com)journal homepage: [www.elsevier.com/locate/watres](http://www.elsevier.com/locate/watres)

# Threshold concentrations of biomass and iron for pressure drop increase in spiral-wound membrane elements

W.A.M. Hijnen\*, E.R. Cornelissen, D. van der Kooij

KWR Waterycycle Research Institute, PO Box 1072, 3430 BB Nieuwegein, The Netherlands

## ARTICLE INFO

### Article history:

Received 27 October 2010

Received in revised form

26 November 2010

Accepted 29 November 2010

Available online 7 December 2010

### Keywords:

Spiral-wound membranes

Biofouling

NPD

Biomass

ATP

Carbohydrates

Fe

Threshold values

## ABSTRACT

In a model feed channel for spiral-wound membranes the quantitative relationship of biomass and iron accumulation with pressure drop development was assessed. Biofouling was stimulated by the use of tap water enriched with acetate at a range of concentrations (1–1000  $\mu\text{g Cl}^{-1}$ ). Autopsies were performed to quantify biomass concentrations in the fouled feed channel at a range of Normalized Pressure Drop increase values (NPD<sub>i</sub>). Active biomass was determined with adenosinetriphosphate (ATP) and the concentration of bacterial cells with Total Direct Cell count (TDC). Carbohydrates (CH) were measured to include accumulated extracellular polymeric substances (EPS). The paired ATP and CH concentrations in the biofilm samples were significantly ( $p < 0.001$ ;  $R^2 = 0.62$ ) correlated and both parameters were also significantly correlated with NPD<sub>i</sub> ( $p < 0.001$ ). TDC was not correlated with the pressure drop in this study. The threshold concentration for an NPD<sub>i</sub> of 100% was 3.7 ng ATP  $\text{cm}^{-2}$  and for CH 8.1  $\mu\text{g CH cm}^{-2}$ . Both parameters are recommended for diagnostic membrane autopsy studies. Iron concentrations of 100–400  $\text{mg m}^{-2}$  accumulated in the biofilm by adsorption were not correlated with the observed NPD<sub>i</sub>, thus indicating a minor role of Fe particulates at these concentrations in fouling of spiral-wound membrane.

© 2010 Elsevier Ltd. All rights reserved.

## 1. Introduction

Microbial growth ('biofouling') in high pressure spiral-wound (SW) membranes for nanofiltration (NF) or reverse osmosis (RO) has been identified as a major cause of operational problems such as increased feed channel pressure drop (PD), decreased mass transfer coefficient (MTC) and product quality decline. First studies on biofouling date from the 1970s and 1980s of the twentieth century (Bailey and Jones, 1974; Potts et al., 1981; Ridgway et al., 1985) and a number of reviews on this issue have been published in the 1990s (Flemming, 1997; Flemming

et al., 1993a; Ridgway and Flemming, 1996) because of the increasing application of membrane processes in water treatment and desalination. Destructive membrane sampling (autopsies) has been used to analyze the composition and structure of accumulated biofilms in order to elucidate the fundamentals of the biofouling process in spiral-wound membranes. With different microscopic techniques membrane foulants have been detected and identified as bacterial matter (Ridgway and Flemming, 1996). Still there is a lack of information on the quantitative relationship between biomass concentrations and the resulting operational problems in

**Abbreviations:** AOC, assimilable organic carbon; ATP, Adenosinetriphosphate; CH, carbohydrates; EPS, extracellular polymeric substances; FS, feed spacer; HPC, heterotrophic colony plate count; IPC, ion chromatography; NF, nanofiltration; NPD, normalized pressure drop; MFS, membrane fouling simulator; MTC, mass transfer coefficient; PD, pressure drop;  $R_f$ , exponential fouling rate constant; RO, reversed osmosis; SW, spiral-wound; TDC, total direct cell count.

\* Corresponding author.

E-mail address: [wim.hijnen@kwrwater.nl](mailto:wim.hijnen@kwrwater.nl) (W.A.M. Hijnen).

0043-1354/\$ – see front matter © 2010 Elsevier Ltd. All rights reserved.

doi:10.1016/j.watres.2010.11.047

NF/RO membranes. Such information is not only needed for diagnostic purposes and improvement of pretreatment but also for assessing the efficacy of cleaning procedures to control biofouling.

Microbial analysis such as Heterotrophic Plate Counts (HPC) and Total Direct Cell counts (TDC), and physical and (bio) chemical analysis including total wet weight of deposits, adenosinetriphosphate (ATP), extracellular polymeric substances (EPS) and proteins have been used to measure the amount of biomass on SW membranes (Flemming and Schaule, 1988; Griebel and Flemming, 1998; Ridgway et al., 1983; Schaule et al., 1993; Vrouwenvelder et al., 1998; Vrouwenvelder et al., 2008). Only few studies have tried to establish quantitative relationships between these biomass parameters and the pressure drop or flux decline. Flemming et al. (1993b) observed an MTC decline of 25% at total cell coverage of the membrane surface of  $5 \times 10^7$ – $2 \times 10^8$  cells  $\text{cm}^{-2}$  and suggested a 'pain level' of bacterial cells of  $10^8$  per  $\text{cm}^2$ ; no correlation with pressure drop was presented. This 'pain level' corresponds with the amount of bacterial cells observed in SW membranes with operational problems related to biofouling (Griebel and Flemming, 1998; Hijnen et al., 2009; Schaule et al., 1993; Vrouwenvelder et al., 1998). Measuring active bacterial biomass with ATP in cell cultures or biomass samples is attractive because the analytical method is rapid, cheap and simple to perform and has a low detection level; a concentration of  $1 \text{ ng l}^{-1}$  ATP can be detected without concentration techniques. The proportional relationship between ATP and TDC (Magic-Knezev and Van der Kooij, 2004; Vrouwenvelder et al., 2008) indicates that ATP is a potential parameter to quantify the amount of accumulated biomass. Furthermore, autopsy results from full-scale SW membrane installations showed that the increase of the Normalized Pressure Drop (NPD) was related to ATP concentrations (Vrouwenvelder et al., 2008). However, establishment of a causal relationship between ATP and NPD requires more defined conditions to exclude effects of other deposits (dead biomass, EPS and other organic or inorganic substances). Quantification of carbohydrates (CH) with the Dubois method (Dubois et al., 1956) in autopsy studies enables to estimate biomass concentrations based on EPS which consists of polysaccharides with a large water-retention capacity resulting in voluminous deposits. The Dubois method is commonly used in membrane autopsy studies (Gabelich et al., 2004; Griebel and Flemming, 1998; Ridgway et al., 1983) and correlated with flux decline (Fonseca et al., 2007). Biofouling rarely occurs without mineral deposition (Ridgway and Flemming, 1996) and Fe was identified as a predominating foulant in SW elements (Baker and Dudley, 1998), but a causal relationship between Fe and PD increase was not reported. Hence, evaluation of the use of ATP, TDC and CH as quantitative biomass parameters in diagnostic autopsies and cleaning studies as well as elucidation of the role of Fe in pressure drop problems requires biofouling studies under well defined conditions.

In a recent laboratory study using a Membrane Fouling Simulator (MFS) (Vrouwenvelder et al., 2006) a quantitative relationship between acetate as a model substrate and the pressure drop increase was demonstrated (Hijnen et al., 2009). Samples of the biofouled membranes were available for autopsy studies. The objectives of the current study were:

(i) elucidation of the quantitative relationship between biomass parameters ATP, TDC and CH and the extent of the PD increase and (ii) determination of the threshold concentrations of these parameters for a 100% increase of the normalized pressure drop (NPD) and (iii) to investigate the role of iron as the major mineral in the water under the experimental conditions. Such information enables the selection of proper biomass parameter(s) in autopsies to assess the cause of PD in membrane elements.

## 2. Materials and methods

### 2.1. Biofouling of an NF membrane

The Membrane Fouling Simulator (MFS) loaded with sheets ( $7 \times 30 \text{ cm}$ ) of a "virgin" nanofiltration membrane sheet (Trisep 4040-TS80-TSF) was supplied with non-chlorinated tap water after filtration (10 and  $1 \mu\text{m}$  poly-propylene cartridge filtration; Van Borselen Ltd.) to exclude accumulation of suspended solids and spiked with low amounts of acetate-C to initiate biofouling. These experiments have been described in detail (Hijnen et al., 2009). Briefly, the MFS is a small scale continuous flow model of an SW feed channel ( $0.8 \times 4 \times 22 \text{ cm}$ ) filled with the matching Trisep feed spacer ( $0.8 \times 4 \times 20 \text{ cm}$ ; front 2 cm without feed spacer FS) and operated at a constant feed water flow of  $16 \text{ l h}^{-1}$  (cross-flow velocity of  $0.14 \text{ m s}^{-1}$ ) at a constant pressure of 1 bar without permeation. Fig. 1 depicts the experimental set up. The rate of clogging of the feed channel was measured by monitoring the pressure drop normalized (NPD) to a moderate environmental temperature of  $12.5^\circ\text{C}$  in the feed channel (Hijnen et al., 2009). The extent of biofouling, given by the relative NPD increase ( $\text{NPD}_i$ ), is calculated from the final NPD ( $\text{NPD}_f$ ) and the initial NPD ( $\text{NPD}_0$ ) by

$$\% \text{NPD}_i = \frac{\text{NPD}_f - \text{NPD}_0}{\text{NPD}_0} \cdot 100\% \quad (1)$$

The MFS units were supplied with pre-filtered tap water spiked with acetate-C at concentrations ( $S_{\text{ac}}$ ) of 1, 3, 5, 10, 25, 100, 500 and  $1000 \mu\text{g l}^{-1}$ . Four blank MFS units with no acetate supply were operated with either filtered tap water or unfiltered tap water.

### 2.2. Feed water quality

The feed water was non-chlorinated tap water produced from anaerobic groundwater using aeration and rapid sand filtration. The pH of the water was  $7.98 \pm 0.05$ , dissolved organic carbon content was  $2.0 \pm 0.1 \text{ mg C l}^{-1}$ , assimilable organic carbon concentration (AOC) was  $3\text{--}5 \mu\text{g acetate-C eq l}^{-1}$ ,  $\text{NO}_3^-$  and  $\text{PO}_4^{3-}$  content was  $0.12 \pm 0.04$  and  $0.02 \pm 0.02 \text{ mg l}^{-1}$  respectively. The iron content (ion chromatography; ICP method with a lower detection limit of  $0.005 \text{ mg l}^{-1}$ ) of the filtered tap water was  $0.008 \pm 0.014 \text{ mg l}^{-1}$  and  $0.32 \pm 0.24 \text{ mg l}^{-1}$  in the unfiltered tap water. Iron was the major mineral in the tap water and visually (brown deposits) accumulated in the biofilms. The ambient water temperature was daily monitored during the experiments and ranged from  $13.5$  to  $16.8^\circ\text{C}$  (average of  $15.9 \pm 0.7^\circ\text{C}$ ) and was  $19.4 \pm 2.0^\circ\text{C}$  in one experiment.

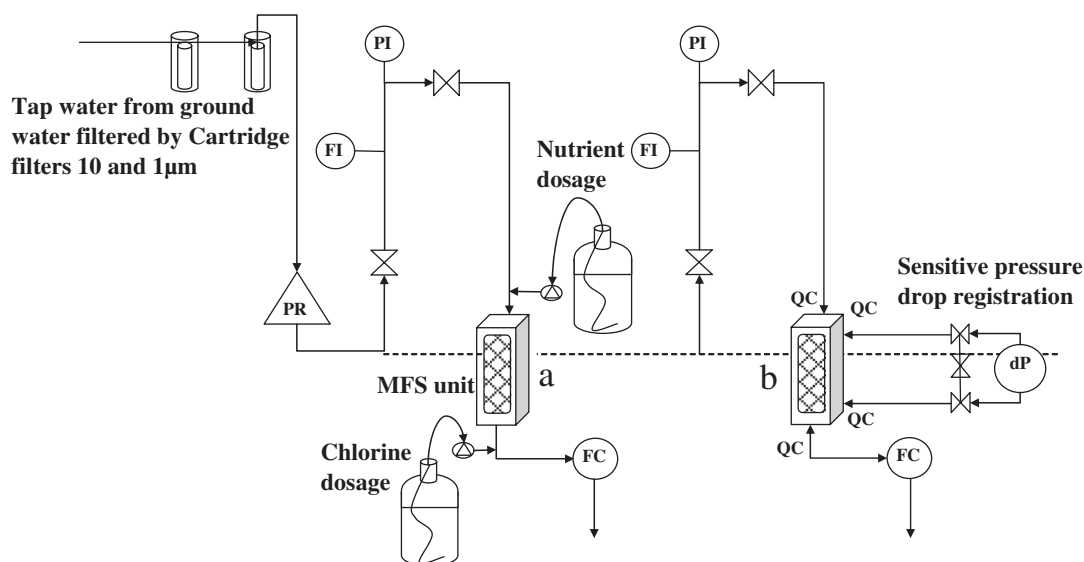


Fig. 1 – Experimental set up for the experiments with a total of five MFS units. Unit on the left with dosage equipment and unit on the right with the mobile pressure drop monitor; PI and FI = pressure and flow indicator; FC = flow controller; QuC = quick connector.

### 2.3. Autopsy of the membrane sheets

Two samples ( $1.5 \times 2$  cm) were cut from the membrane at the inlet section of the feed channel without spacer (no FS) and five samples ( $2 \times 2$  cm) were cut from the membrane with spacer. The samples were transferred to sterile glass tubes with 20 ml of autoclaved tap water and sonicated with High Energy Sonication (HES, #100) using a BRANSON Digital Sonifier (Model 250 D) at optimized conditions established in a previously published study (Magic-Knezev and Van der Kooij, 2004). The sonifier tip (size 6.5 mm) was inserted into the tube (1–2 cm) containing 20 ml of autoclaved water and the membrane/spacer sample. This tube was placed in melting ice and sonicated for one minute at an amplitude of 45% (15–20 watt) to separate the biomass from the membrane/spacer samples. This treatment was repeated in 20 ml fresh sterile tap water and both suspensions were mixed to obtain a total sample volume of 40 ml. The biomass samples of the experiments with  $S_{ac}$  of 25, 3 and  $1 \mu\text{g l}^{-1}$  were collected by additional swabbing to enlarge the biomass recovery. The swab was treated with HES for 1 min in 20 ml autoclaved tap water and subsequently mixed with the 40 ml HES suspension.

### 2.4. Microbial parameters

ATP was measured to determine the amount of active bacterial biomass in the biofilm samples. The analysis is based on measuring the amount of light produced by an enzymatic reaction using the luciferine–luciferase assay in a luminometer (Celcis Ltd.) and has a lower limit of detection of  $1 \text{ ng l}^{-1}$ , which corresponds with  $0.01 \text{ ng cm}^{-2}$  of membrane surface. The method has been described in detail previously (Magic-Knezev and Van der Kooij, 2004). The total direct cell count (TDC) was based on counting of fluorescing cells using epifluorescence microscopy (Hobbie et al., 1977) and

the analytical procedure was described in detail before (Hijnen et al., 2009). The detection limit is  $180 \text{ cells ml}^{-1}$ , which corresponds to  $720 \text{ cells cm}^{-2}$ .

### 2.5. Carbohydrate analysis

The CH concentration in the biofilm samples was analyzed with the method described by Dubois et al. (1956) using glucose as the reference carbohydrate. The extinction/adsorption at 490 nm was measured directly in the biomass suspension after hydrolysis and complexation with sulphuric acid and phenol, respectively and expressed in glucose equivalent concentration. The detection limit of this parameter was approximately  $5\text{--}10 \mu\text{g cm}^{-2}$  depending on the sampled membrane area.

### 2.6. Iron content

The iron (Fe) content of the obtained biomass suspension was assessed with Atomic Absorption Spectrometry resulting in a lower limit of detection of approximately  $1 \text{ mg cm}^{-2}$  of membrane surface.

### 2.7. Correlation analysis and statistics

Correlation analyses was done by determining Pearson's correlation coefficient between paired values of ATP, TDC, CH and Fe using SPSS 17.0 software with a significance level of  $p \leq 0.01$ . For the correlation of the biomass and Fe accumulated in the MFS units with the NPD increase (%), the weighted average concentrations ( $\bar{C}_{avg}$ ) were calculated from the concentrations observed in the samples at different locations in the MFS units using

$$\bar{C}_{avg} = \frac{\sum_{i=1}^n (C_i + C_{i+n}) / 2 * A_{i+n}}{A_{tot}} \quad (2)$$

where  $C_i$ ,  $C_{i+n}$  and  $A_{i+n}$  ( $\text{cm}^{-2}$ ) are the concentration and the surface area at the  $i$ th part of  $n$  parts of the feed channel surface ( $n=3-7$ ) and  $A_{\text{tot}}$  is the total surface area of the MFS unit. The linear regression analysis of the correlation between the  $\bar{C}_{\text{avg}}$ -values of the biomass parameters and Fe concentrations obtained from membrane autopsy and the  $\text{NPD}_i$  was performed with Excel software. For the correlation of the biomass parameters and Fe concentrations with the  $\text{NPD}_i$  the non-parametric Spearman's rank correlation coefficient was calculated and multi-regression analysis was conducted with SPSS 17.0 software.

### 3. Results

#### 3.1. NPD increase

In the MFS units supplied with acetate-enriched tap water biofouling was observed at each concentration (Fig. 2) and the NPD increase ( $\text{NPD}_i$ ) was characterized as a first order process (Hijnen et al., 2009). The blank MFS unit supplied with pre-filtered tap water without added acetate showed no  $\text{NPD}_i$  during 28 days of operation (Fig. 2a), whereas in units supplied with  $1 \mu\text{g}$  of acetate-C/l biofouling was observed (Fig. 2b). Also no fouling was observed within 100 days of operation in the two blank units supplied with unfiltered water (Fig. 2c). After 100 days the pressure drop started to increase in these units. The accumulated biofilm in the feed channels was colourless at high biofouling rates and short operation times ( $<20$  days). At lower biofouling rates and operational times of  $\geq 25$  days the feed channel showed accumulation of brown coloured deposits. These observations initiated the analysis of the Fe concentrations in the fouled membrane samples.

#### 3.2. Spatial distribution of biomass and Fe

The units were sampled for biomass and Fe concentrations at different fouling conditions with relative  $\text{NPD}_i$  values ranging from 71 to 3390% (Table 1). The MFS units supplied with acetate showed high ATP concentrations at the inlet section without spacer (no FS), further elevated concentrations in the first part of the section with feed spacer (0–2 cm) and a decline

of concentrations in the subsequent parts of the channel (Fig. 3). In the units supplied with acetate the percentage of the total amount of ATP at the inlet section (no FS) was 1.5–9%, in the first 2 cm with feed spacer 8–16% and in the last part (18–20 cm) 3–10% (Fig. 3c). At acetate concentrations of 1000, 500 and  $25 \mu\text{g Cl}^{-1}$  the ATP concentrations were higher than in the units supplied with the lower acetate concentrations (10, 5, 3 and  $1 \mu\text{g Cl}^{-1}$ ). In the blank MFS units without acetate dosing a lower ATP concentration was observed (Fig. 3b). The spatial distribution of parameters TDC and CH and also of Fe in the channels was similar to the distribution of ATP; a declining concentration in the section with feed spacer (no figures presented; weighted average concentrations presented in Table 1).

#### 3.3. Correlation analysis of biomass parameters and iron

The operational periods with acetate dosing, the final  $\text{NPD}_i$  values and the exponential fouling rate constant  $R_f$  and the weighted average values ( $\bar{C}_{\text{avg}}$ ) of the biomass parameters and Fe for the correlation analysis are presented in Table 1. The correlation analysis of the paired biomass parameters showed that the log value of the ATP concentration in the MFS units was significantly ( $p < 0.01$ ) correlated with the log value of the TDC and the CH concentrations, respectively (Table 2). The linear regression equation for the relationship with TDC was  $\text{Log} [\text{ATP}] = 0.79$  (95% CI 0.69–0.89)  $\text{Log} [\text{TDC}] + 4.1$  (95% CI 3.6–4.6) with a goodness of fit ( $R^2$ ) of 0.75. Based on this correlation 1 ng of ATP equals  $3 \times 10^6$  (95% CI  $5.3 \times 10^5$ – $1.7 \times 10^7$ )  $\text{TDC cm}^{-2}$ . The CH concentration ranged between 10 and  $100 \mu\text{g cm}^{-2}$  at ATP concentrations of 10–100  $\text{ng cm}^{-2}$ , but the linear regression fit of paired ATP and CH values was poor ( $R^2 = 0.39$ ). A better fit ( $R^2 = 0.62$ ;  $p < 0.0001$ ) was observed for the values of the units operated under acetate limitation conditions where the fouling rate  $R_f$  was below  $R_{f,\text{max}}$  ( $S_{\text{ac}} \leq 10 \mu\text{g l}^{-1}$ ). ATP and Fe concentrations were not correlated when the results of the MFS units operated at high  $S_{\text{ac}}$  values with relatively short operation times ( $\leq 20$  days) were included. For the MFS units operated at  $S_{\text{ac}}$  values  $\leq 10 \mu\text{g l}^{-1}$  with longer operational periods ATP and Fe concentrations were significantly correlated ( $p < 0.001$ ; Table 2). TDC did not correlate with CH and Fe. The latter two parameters correlated significantly ( $p < 0.001$ ) with a better

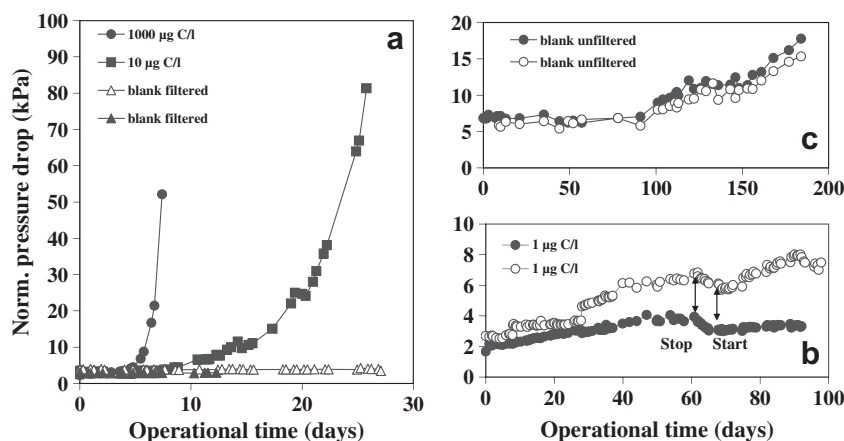


Fig. 2 – The development of the Normalized pressure drop (NPD) in the MFS units supplied with filtered tap water enriched with different acetate concentrations (a,b) and (c) supplied with unfiltered tap water (lines in b and c are duplicates).



**Table 1 – The fouling conditions of the MFS experiments and the weighted average concentration ( $\bar{C}_{avg}$ ) of the biomass parameters and iron measured by autopsies.**

Acetate $S_{ac}$ ( $\mu\text{g C/l}$ )	Operational time (days)	Final pressure drop (kPa)	% NPD increase	$R_f^b$ ( $\ln \text{NPD}_i \text{ d}^{-1}$ )	ATP ( $\text{ng cm}^{-2}$ )	TDC ( $\text{cell} \times 10^8 \text{ cm}^{-2}$ )	CH ( $\mu\text{g gluc. eq cm}^{-2}$ )	Fe ( $\text{mg m}^{-2}$ )
0 pre-filtered	20	2.9	6.0	<0.001	0.8	0.02	9.4	0.32
0 unfiltered	184; 184	17.8; 15.3	156; 157	0.015; 0.016	3; 2	0.3; 0.4	9.6; 10.0	394; 298
1	146; 98	3.3; 7.2	71; 119	0.063; 0.027	6; 3	Nd <sup>d</sup> ; 0.1	Nd <sup>e</sup>	96; 129
3	34; 152	18.6; 24.5	306; 526	0.102; 0.109	20; 18	2.0; 2.3	Nd <sup>e</sup>	83; 173
5	39; 46	15.7; 37.9	376; 919	0.128; 0.245	16; 13	0.3; 0.4	11.7; 11.9	149; 212
10	35; 28	7.9 <sup>c</sup> ; 81.4	234 <sup>c</sup> ; 2369	0.205; 0.224	28; 46	0.3; 0.6	13.0; 44.6	201; 426
25	35; 33	37.8; 54.7	1352; 993	0.766; 0.696	175; 158	1.4; 0.5	Nd <sup>e</sup>	82; 79
500	20; 15	61.3; 22.2	3390; 507	0.859; 1.144	200; 91	2.2; 3.1	52.4; 20.6	11; 1
1000	15; 14; 8	52.1; 18.4; 7.9	1820; 445; 182	1.126; 1.475; 1.097	118; 58; 184	1.0; 1.2; 1.4	21.1; 14.4; 47.1	1; nd; 7
S1 <sup>a</sup>	31	46.1	725	100: 1.123	37	0.5	21.3	334
S2 <sup>a</sup>	53	45.4	1231	1000: 1.160	37	0.8	37.3	154

a Starvation experiments with variable acetate dosages and starvation periods (S1 = 100–5 and S2 = 1000–1000–10) (Hijnen et al., 2009).

b First order fouling rate  $R_f$  values from Hijnen et al. (2009) modified as submitted in an erratum (Hijnen et al., in press).

c Low NPD<sub>i</sub> caused by preferential flow path in the feed channel.

d Nd = not determined.

e Unreliable CH data due to the use of cotton swab.

goodness of fit for the units with acetate-C concentrations of  $\leq 10 \mu\text{g l}^{-1}$  (Table 2).

### 3.4. Correlation with NPD<sub>i</sub>

The study aimed at assessing the relationship between the biomass concentration and Fe with the NPD<sub>i</sub> at the time of the autopsy. The weighted average ATP and CH concentrations in the MFS units were both significantly ( $p < 0.01$ ) correlated to the NPD<sub>i</sub> (%) as evaluated with the non-parametric Spearman's rank correlation coefficient ( $R^2$  of 0.71 and 0.91, respectively). The linear regression analysis also showed a significant ( $p < 0.001$ ) correlation with a high correlation coefficient for

ATP and CH (0.52, 0.70 and 0.82; Table 2 and Fig. 4). No significant correlation was observed for TDC with NPD<sub>i</sub> (Fig. 4c). The variability of ATP and CH concentrations in the MFS units is presented in Fig. 4 with the standard deviation (s.d.;  $n = 3-7$ ). The bars show an increased variability of both parameters at increased NPD<sub>i</sub> values which was caused by increased heterogeneity of the concentrations in the feed channel (Fig. 3).

No correlation was found between the concentrations of Fe and the NPD<sub>i</sub> values (Fig. 4c), but the regression plots of ATP and CH with NPD<sub>i</sub> revealed that the low ATP and CH concentration at relatively high NPD<sub>i</sub> values contained Fe concentrations of  $>100-200 \text{ mg m}^{-2}$ . However, a multi-regression analysis in combination with either ATP or CH again showed

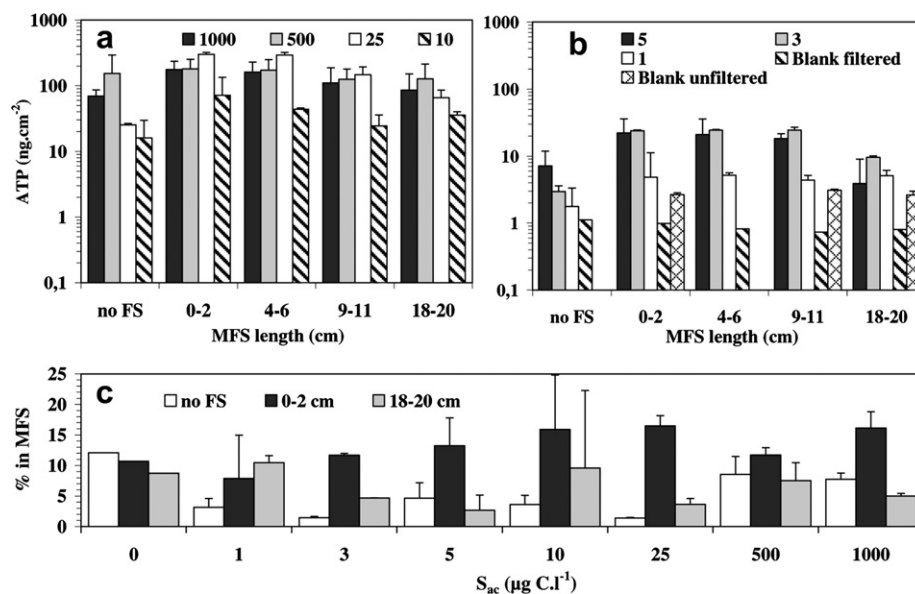


**Fig. 3 – Distribution of ATP concentrations (error bar is s.d.) in the MFS units supplied with filtered tap water enriched with different acetate-C concentrations ( $\mu\text{g l}^{-1}$ ) and with unfiltered tap water (a,b) and (c) % of the total ATP amount in the membrane feed channel without feed spacer (no FS) and after 0–2 and 18–20 cm with feed spacer.**

**Table 2 – Correlation matrix of the different biomass parameters, Fe and NPD<sub>i</sub> measured in the standard MFS experiments; presented are the square of the Pearson correlation coefficient  $R^2$ , for all correlations  $p$ -values were  $< 0.001$  except for values indicated by \* ( $p$ -value  $< 0.01$ ), the number of observations ( $n$ ).**

	$S_{ac}$ values ( $\mu\text{g CL}^{-1}$ )	TDC (cells $\text{cm}^{-2}$ )	CH ( $\mu\text{g cm}^{-2}$ )	Fe ( $\text{mg m}^{-2}$ )	NPD <sub>i</sub> <sup>c</sup> (%)
ATP ( $\text{ng cm}^{-2}$ )	1–1000 $\leq 10$	0.75; 85 <sup>a</sup> 0.66; 43 <sup>a</sup>	0.39; 49 0.62; 30	nc <sup>b</sup> ( $p = 0.09$ ) 0.56; 42	0.52; 19 0.70*; 9
TDC (cells $\text{cm}^{-2}$ )	1–1000	1	nc	nc	nc
CH ( $\mu\text{g cm}^{-2}$ )	1–1000 $\leq 10$		1	0.34; 30 0.65; 16	0.82; 13
Fe ( $\text{mg m}^{-2}$ )	1–1000			1	nc

a Log transformed values.  
b Nc = no correlation.  
c Correlation with the weighted average concentrations of the parameters.

no significant correlation between Fe and NPD<sub>i</sub>. This indicates that the contribution of Fe accumulation in the MFS units to the pressure drop increase was limited. The minor effect of the Fe concentrations on the NPD<sub>i</sub> was also demonstrated by the Fe content in the MFS units supplied with unfiltered tap water (unfiltered blanks; Fig. 4c). The Fe concentrations in these unfiltered blanks with a limited NPD<sub>i</sub> of 156% were 298 and 394  $\text{mg m}^{-2}$ , whereas ATP and CH concentrations were low (2–3  $\text{ng cm}^{-2}$  and 9.6–10  $\mu\text{g cm}^{-2}$ , respectively; Table 1). In the MFS units at  $S_{ac}$  value of 10  $\mu\text{g L}^{-1}$  considerably higher NPD<sub>i</sub> values (234–2369%) were observed at comparable Fe content of 201–426  $\text{mg m}^{-2}$  and higher biomass concentrations of 28–46  $\text{ng ATP cm}^{-2}$  and 13–44.6  $\mu\text{g CH cm}^{-2}$ . Similar observation was recorded for the MFS unit supplied with 100 and 5  $\mu\text{g L}^{-1}$  acetate and intermediate starvation period; Fe, ATP and CH content was 334  $\text{mg m}^{-2}$ , 37  $\text{ng cm}^{-2}$  and 21.3  $\mu\text{g cm}^{-2}$ , respectively at an NPD<sub>i</sub> of 725%.

The pressure drop increase was due to a decrease of the open pore volume of the feed channel which in turn was a result of biomass accumulation. The relationship between the biofilm thickness and the NPD<sub>i</sub> has been described with hydraulic equations (Schock and Miquel, 1987) and is linear in the initial stage of biofouling but exponential in the subsequent stage (Hijnen et al., 2009). Assuming that ATP and CH

concentrations were linearly related with the biofilm thickness the correlations with NPD<sub>i</sub> were also tested for an exponential relationship. Both exponential fits were significant ( $p < 0.01$ ), but the goodness of fit was lower compared to the linear regression (Fig. 4).

### 3.5. Threshold concentrations

The ATP concentration in the feed channels of the MFS units for an NPD<sub>i</sub> of 100% was 3.7  $\text{ng cm}^{-2}$  ( $\pm 95\%$  CI = 1.3–10.9), calculated from the equation presented in Fig. 4a. For CH the threshold concentration for this criterion was calculated from the equation given in Fig. 4b at 8.1  $\mu\text{g cm}^{-2}$  ( $\pm 95\%$  CI of 6.1–11.7). This was around the detection limit of the analysis of 5–10  $\mu\text{g cm}^{-2}$ . For TDC and Fe no threshold concentration was calculated because of the lack of correlation with NPD<sub>i</sub>.

### 3.6. Fouling and accumulation rate

The fouling rate in the feed channel of the MFS units could be described with the exponential fouling rate constant  $R_f$  (Table 1). Formation of biofilms on surfaces initially is an exponential process that is rapidly followed by a linear phase due to diffusion limitation of the substrate flux into the

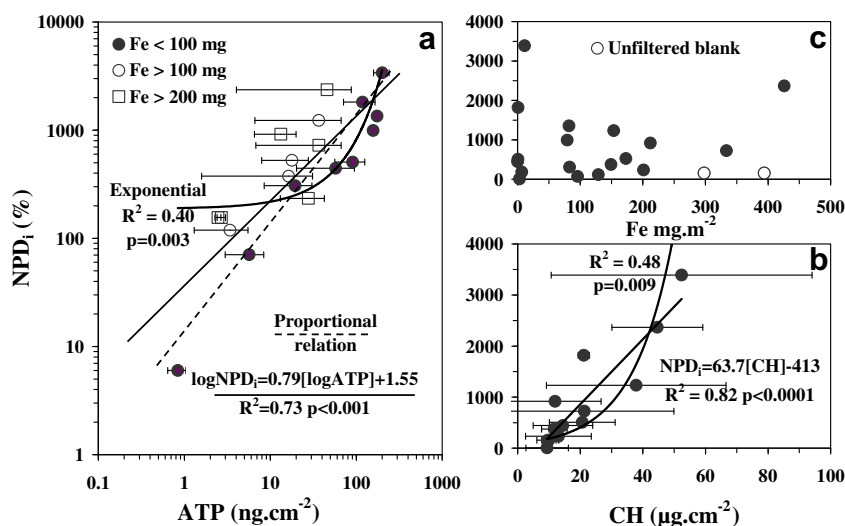


**Fig. 4 – The relationship between the accumulated biomass measured with ATP and CH (a,b) and (c) the accumulated mass of Fe with the NPD<sub>i</sub> (%); error bar is s.d. ( $n = 4-7$ ).**

biofilm (Rittmann, 1995). This was clearly demonstrated for ATP and Fe accumulation on glass (Van der Kooij et al., 2003). On base of the concentrations of ATP, CH and Fe measured in the MFS units after the different dosing periods the linear accumulation rate of these parameters was calculated and correlated with the  $S_{ac}$  in the influent and  $R_f$  (Fig. 5a). Correlations of both biomass parameters with  $S_{ac}$  showed a similar saturation curve and relationship with  $S_{ac}$  as described for  $R_f$  (Fig. 5a). The ATP and CH accumulation rates were strongly correlated ( $p < 0.0001$ ) with  $R_f$  with  $R^2$  of 0.91 for ATP and 0.90 for CH. This clearly demonstrates the proportional relationship of both biomass parameters with the porosity decline in the feed channel.

## 4. Discussion

### 4.1. ATP and TDC as biomass parameters in autopsies

In full-scale SW membrane filtration installations where operation is hampered by fouling problems, it is common practice to carry out an autopsy to verify the cause of the fouling process. Only few studies have been published on the quantitative correlation between biomass parameters and operational problems in membranes such as pressure drop increase and flux decline (Flemming et al., 1993b; Fonseca et al., 2007; Vrouwenvelder et al., 2008). The results of the present study show that ATP is a suitable parameter to elucidate the role of biofilm formation in the pressure drop increase in such membranes. This conclusion was based on the correlation with the observed NPD<sub>i</sub> and supported by the good correlation between the biofilm formation rate (ng ATP cm<sup>-2</sup> d<sup>-1</sup>) in the feed channel of the MFS with the acetate concentration (Fig. 5a) and the exponential fouling rate constant  $R_f$  (Fig. 5b). Additionally, this clearly shows that the assessment of the biofilm formation rate for the feed water of SW membranes which is also based on ATP measurements (Van der Kooij et al., 2003) is an appropriate parameter to assess the biofouling potential of the feed water.

The choice of a 100% NPD<sub>i</sub> in the current study to assess a threshold biomass concentration was based on a commonly used NPD<sub>i</sub> cleaning criterion of 15% over one stage of a series of six successive membrane elements (Graham et al., 1989; Hickman, 1991; Speth et al., 1998). The NPD<sub>i</sub> is not evenly distributed over the elements and usually is mainly located in the first element. Consequently, the NPD<sub>i</sub> in this element is higher (Vrouwenvelder et al., 2009a) and may be close to 100%. The threshold ATP concentration for 100% NPD<sub>i</sub> in the MFS units was 3.7 ng cm<sup>-2</sup>. A higher threshold ATP concentration for 100% NPD<sub>i</sub> of 30 ng cm<sup>-2</sup> was reported for SW elements operated under field conditions (Vrouwenvelder et al., 2008). However, one would expect this the other way around: lower for the same NPD<sub>i</sub> in the field elements because of differences in biofilm conditions. MFS units of the present study contained relatively young biofilms whereas biofilms in field elements were more aged with a lower ratio between active (ATP) and total biomass (including EPS and dead cell material). This difference between threshold values might be caused by the difference in 100% NPD<sub>i</sub> over SW elements and the MFS of the current study. It can also be caused by correlating on one hand the maximum ATP concentration with the NPD<sub>i</sub> in field elements with a length of 1 m (Vrouwenvelder et al., 2008) and on the other hand the weighted average ATP concentration with the NPD<sub>i</sub> in a 0.2 m feed channel of the MFS as done in the present study. Consequently, despite the positive correlations ATP results in field autopsies must be interpreted with care and additional parameters which are more related to the total amount of the accumulated biomass are needed.

The present study and also the mentioned field study (Vrouwenvelder et al., 2008) revealed that in contrast to ATP, TDC was not correlated with NPD<sub>i</sub>. The range of TDC values of  $1 \times 10^7$ – $3.1 \times 10^8$  corresponds with a biofilm thickness of 0.1–1.6 μm (assumed bacteria cell volume of 0.5 μm<sup>3</sup>; diameter of 1 μm). Theoretically for the 100% NPD<sub>i</sub> a biofilm thickness of 60 μm was estimated (Hijnen et al., 2009) thus indicating that microscopic cell count (TDC) is not an accurate parameter for total biomass and more importantly biofilms consist of more than bacterial cells.

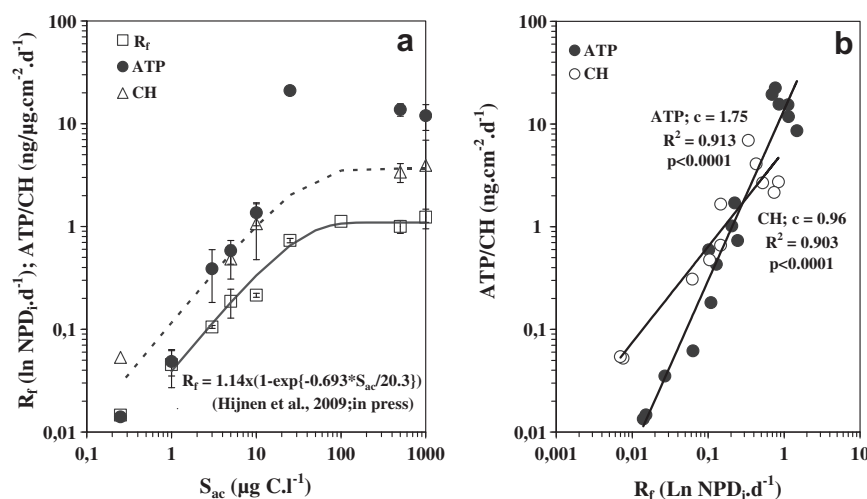


Fig. 5 – The correlation of the exponential fouling rate  $R_f$  and the ATP and CH accumulation rates with the acetate concentrations  $S_{ac}$  (a) and (b) the correlation of the biomass (ATP/CH) accumulation rates with  $R_f$ .

#### 4.2. Carbohydrates as a biomass parameter

Biofilms are established by adsorption and adherence of bacteria followed by growth due the supply of nutrients. Extracellular polymeric substances (EPS) excreted by bacteria to anchor themselves to the surface and to each other play a key role in the development of biofilms (i.e. protection against environmental stress, nutrient availability; Or et al., 2007; Flemming and Wingerden, 2010). CH are important components of EPS (Sutherland, 1999). The method of Dubois et al. (1956) is commonly applied to quantify the CH concentration in field SW elements (Gabelich et al., 2004; Griebel and Flemming, 1998; Ridgway et al., 1983, 1984) and their reported CH concentrations were in the same order of magnitude as measured in the current study. The positive correlation between the CH concentration and pressure drop in the feed channel of the MFS (Fig. 4b) and the proportional correlation of the CH accumulation rate ( $\mu\text{g cm}^{-2} \text{d}^{-1}$ ) to the exponential fouling rate the  $R_f$  (Fig. 5b) confirms that the CH concentration in SW membranes is a valuable parameter in diagnostic autopsies. The threshold CH concentration of  $8.1 \mu\text{g cm}^{-2}$  for the defined NPD<sub>i</sub> was around the current detection limit of the analysis, but the analysis can be optimized by sampling larger surface areas. More recently the CH parameter was correlated with flux decline in NF membranes (Fonseca et al., 2007) and they reported a decline of 30–80% when the CH concentrations increased to  $50 \mu\text{g cm}^{-2}$ . Another study presented a >50% flux decline and 100% NPD increase in SWM elements at a CH concentration of  $12.4 \mu\text{g cm}^{-2}$  (Gabelich et al., 2004). Consequently, we propose the use of the parameters ATP and CH in membrane autopsy studies: the ATP method which is cheap and fast and reveals information on the accumulated active biomass in the feed channel and CH which represents the total amount of active and inactive biomass. Inclusion of the analysis of CH is especially of interest for studies on the effect of membrane cleaning with chemicals (Cornelissen et al., 2009).

#### 4.3. Fe accumulation and pressure drop increase

In the flat sheet MFS units without permeate production the process of particulate accumulation on the membrane surface was not influenced by vertical forces and particle settling which normally occur in SW elements with permeate production (Belfort and Nagata, 1985; Belfort, 1988). Thus, the observed accumulation of Fe particles in the MFS was a result of adsorption of these particles onto biomass produced on the membrane surface during the short cross-flow contact time. The results of the current study show that the accumulation of biomass has a far greater effect on NPD<sub>i</sub> in the feed channel than the accumulation of Fe particulates (Fig. 4c). In the units supplied with unfiltered tap water lower biofilm concentrations were observed than in the units supplied with  $1 \mu\text{g}$  acetate-CL<sup>-1</sup> (Fig. 3) but the Fe content was much higher at similar NPD<sub>i</sub> values (71–157%; Table 1). The significant correlation between CH and Fe (Table 2) indicates that EPS plays a substantial role in the adsorption of Fe onto charged biopolymers which is related to the presence of negatively charged carboxylic and phosphate groups (Wuertz et al., 2001). The dominant role of biomass in the NPD<sub>i</sub> is explained by the high water-retention capacity of EPS. Water-retention curves

show that certain polysaccharides hold more than 50–70 g of water per gram while maintaining structural coherence (Or et al., 2007; Chenu, 1993). No studies on the role of Fe particulates in SW membranes on pressure drop are known to the authors. A recent study presented the correlation of the mass deposit of Fe micro- and nanoparticles in a porous sand column ( $208 \text{ cm}^3$ ; empty space volume of  $102 \text{ cm}^3$  and porosity of 0.49) with the pressure drop increase (Vecchia et al., 2009). In this study an Fe concentration of  $2.6 \text{ mg cm}^{-3}$  resulted in a PD<sub>i</sub> in the sand column of 1 kPa. The Fe concentration in the MFS supplied with unfiltered water was 300–400  $\text{mg m}^{-2}$  (Table 2) which equals a volumetric concentration of  $0.41\text{--}0.54 \text{ mg cm}^{-3}$  (channel height of 0.0008 m and porosity of 92%). The %NPD<sub>i</sub> in this MFS was 156–157% with higher ATP and TDC values than in the pre-filtered blank (Table 1). These calculations show that Fe accumulation in the feed channel of SW elements at a level of  $\leq 100 \text{ mg m}^{-2}$  ( $10 \mu\text{g cm}^{-2}$ ) has no effect on the NPD. Further studies under field conditions are required, however, to collect additional data on the relationship of particulate accumulation and biofouling.

#### 4.4. Feed spacer enhances biofilm accumulation

The spacer in the feed channel enhanced biomass accumulation (Fig. 3) which is consistent with observations in other studies (Picioreanu et al., 2009; Vrouwenvelder et al., 2009b). Possible explanations for this observation are: an increase in attachment area or/and enhanced mass transfer of nutrients to the biofilm due to increased turbulence. Based on a specific surface area of the feed spacer of  $7700 \text{ m}^2 \text{ m}^{-3}$  (Picioreanu et al., 2009) it can be estimated that the spacer contributes with around 25% to the attachment surface in the feed channel. An earlier autopsy study on SWM elements from field locations showed more accumulation of biomass (ATP) on the membrane (38–90%) than on the feed spacer (5–62% of the total amount) (Vrouwenvelder et al., 2008). Preferential flow paths shown by Computational Fluid dynamics and filamentous streamers at the spacer junctions (Picioreanu et al., 2009; Vrouwenvelder et al., 2009b) were not observed in the present study. Verification of the role of the feed spacer in biofouling of SWM elements requires further research.

### 5. Conclusions

The effect of biomass accumulation in spiral-wound membranes on pressure drop increase can be elucidated by measuring concentrations of active biomass with adenosine-triphosphate (ATP) and of total biomass with carbohydrates (CH; Dubois, method) in membrane autopsies. There was a significant correlation ( $p < 0.001$ ) between these parameters in the current study. This study also showed a significant ( $p < 0.001$ ) and causal relationship between both parameters and the NPD<sub>i</sub> in a model feed channel. Furthermore, the calculated ATP and CH accumulation rates were highly correlated with the observed exponential fouling rate. Threshold concentrations for 100% NPD<sub>i</sub> were  $3.7 \text{ ng ATP cm}^{-2}$  and  $8.1 \mu\text{g CH cm}^{-2}$ . Because ATP is related to active biomass and CH to the total biomass, monitoring both parameters in autopsies will reveal further information on the metabolic



state of the accumulated biofilm. Iron accumulation in the feed channel was enhanced by the biofilm growth as demonstrated by the significant correlation between CH and Fe concentrations ( $p < 0.001$ ). Iron concentrations of  $\leq 100 \text{ mg m}^{-2}$  ( $10 \mu\text{g cm}^{-2}$ ) of membrane surface did not contribute to pressure drop increase in spiral-wound membranes. The high impact of accumulation of low biomass concentrations on pressure drop increase is attributed to the high water-retention characteristics of polysaccharides in biofilms.

## Acknowledgements

The research was conducted as part of the Joint Research Program of the Dutch Water Supply Companies and in the MEDINA project co-funded by the European Commission under contract number 036997. The excellent technical support by Nanda Berg, Anke Hanzens-Brouwer and Meindert de Graaf from KWR and Amandine Balthazard and David Biraud from the Ecole Nationale Supérieure de Chimie de Mulhouse is greatly appreciated.

## REFERENCES

- Bailey, D.A., Jones, K.M.C., 1974. The reclamation of water from sewage effluents by reversed osmosis. *Wat. Pollut. Control* 74, 353–366.
- Baker, J.S., Dudley, L.Y., 1998. Biofouling in membrane systems – a review. *Desalination* 118, 81–90.
- Belfort, G., 1988. Membrane modules: comparison of different configurations using fluid mechanics. *J. Mem. Sci.* 35, 245–270.
- Belfort, G., Nagata, N., 1985. Fluid mechanics and cross-flow filtration: some thoughts. *Desalination* 53, 57–79.
- Chenu, C., 1993. Clay or sand polysaccharide associations as models for the interface between micro-organisms and soil: water related properties and microstructure. *Geoderma* 56, 143–156.
- Cornelissen, E.R., Hijnen, W.A.M., van der Kooij, D., 2009. Assessment of the efficiency of hydraulic and chemical cleaning for the removal of biomass from surfaces in a laboratory test, Membrane based desalination: an Integrated Approach. EU-China workshop, Qingdao, China.
- Dubois, M., Gilles, K.A., Hamilton, J.K., Rebers, P.A., Smith, F., 1956. Colorimetric method for determination of sugars and related substances. *Anal. Chem.* 23, 350–356.
- Flemming, H.-C., 1997. Reverse osmosis membrane biofouling. *Exp. Thermal Fluid Sci.* 14, 382–391.
- Flemming, H.-C., Schaule, G., 1988. Biofouling of membranes, a microbiological approach. *Desalination* 70, 95–119.
- Flemming, H.-C., Schaule, G., McDonough, R., 1993a. How do performance parameters respond to initial biofilm formation on separation membranes. *Vom Wasser* 80, 177–186.
- Flemming, H.-C., Schaule, G., McDonough, R., 1993b. Permeation properties of biofilms on separation membranes and the problem of biofouling. *J. Membr. Res.* 87, 199–217.
- Flemming, H.-C., Wingender, J., 2010. The biofilm matrix. *Nat. Rev. Microbiol.* doi:10.1038/nrmicro2415.
- Fonseca, A.C., Summers, R.S., Greenberg, A.R., Hernandez, M.T., 2007. Extra-cellular polysaccharides, soluble microbial products, and natural organic matter impact on nanofiltration membranes flux decline. *Environ. Sci. Technol.* 41, 2491–2497.
- Gabelich, C.J., Yun, T.I., Ishida, K.P., Leddy, M.B., Safarik, J., 2004. The effect of naturally occurring biopolymers on polyamide membrane fouling during surface water treatment. *Desalination* 161, 263–276.
- Graham, S.I., Reitz, R.L., Hickman, C.E., 1989. Improving reverse osmosis performance through periodic cleaning. *Desalination* 74, 113–124.
- Griebe, T., Flemming, H.-C., 1998. Biocide-free antifouling strategy to protect RO membranes from biofouling. *Desalination* 118, 153–156.
- Hickman, C.E., 1991. Membrane cleaning techniques, AWWA Seminar Proceedings, Membrane Technologies in the Water Industry, Orlando (US, FL), March 10–13.
- Hijnen, W.A.M., Biraud, D., Cornelissen, E.R., van der Kooij, D., 2009. Threshold concentration of easily assimilable organic carbon in feedwater for biofouling of spiral-wound membranes. *Environ. Sci. Technol.* 43, 4890–4895.
- Hijnen, W.A.M., Biraud, D., Cornelissen, E.R., van der Kooij, D., Erratum: threshold concentration of easily assimilable organic carbon in feedwater for biofouling of spiral-wound membranes. *Environ. Sci. Technol.*, in press.
- Hobbie, J.E., Daley, R.J., Jasper, S., 1977. Use of nuclepore filters for counting bacteria by fluorescence microscopy. *Appl. Environ. Microbiol.* 33, 1225–1228.
- Magic-Knezev, A., Van der Kooij, D., 2004. Optimisation and significance of ATP analysis for measuring active biomass in granular activated carbon filters used in water treatment. *Water Res.* 38, 3971–3979.
- Or, D., Phutane, S., Dechesne, A., 2007. Extracellular polymeric substances affecting pore-scale hydrologic conditions for bacterial activity in unsaturated soils. *Vadose Zone J* 6, 298–305.
- Picioreanu, C., Vrouwenvelder, J.S., van Loosdrecht, M.C.M., 2009. Three-dimensional modeling of biofouling and hydrodynamics in feed spacer channels of membrane devices. *J. Mem. Sci.* 345, 340–354.
- Potts, D., Ahlert, R.C., Wang, S.S., 1981. A critical review of fouling of reversed osmosis membrane. *Desalination* 36.
- Ridgway, H.F., Flemming, H.-C., 1996. Membrane biofouling. In: Malleviall, J., Odendal, P.E., Wiesner, M.R. (Eds.), *Water Treatment Membrane Processes*. McGraw-Hill, New York.
- Ridgway, H.F., Kelly, A., Justice, C., Olson, B.H., 1983. Microbial fouling of reverse-osmosis membranes used in advanced wastewater treatment technology: chemical, bacteriological and ultrastructural analyses. *Appl. Environ. Microbiol.* 45, 1066–1084.
- Ridgway, H.F., Rigby, M.G., Argo, D.G., 1984. Adhesion of *Mycobacterium* sp. to cellulose diacetate membranes used for reverse osmosis. *Appl. Environ. Microbiol.* 47, 61–67.
- Ridgway, H.F., Rigby, M.G., Argo, D.G., 1985. Bacterial adhesion and fouling of reverse osmosis membranes. *J. Am. Water Works Assoc.* 77, 97–106.
- Rittmann, B.E., 1995. Fundamentals and applications of biofilm processes in drinking water treatment. In: Hrubec, J. (Ed.), *The Handbook of Environmental Chemistry*. Springer Verlag, Berlin, Heidelberg, New York, pp. 61–87.
- Schaule, G., Kern, A., Flemming, H.-C., 1993. RO treatment of dump trickling water membrane biofouling: a case history. *Desalination & Water Reuse* 3, 17–23.
- Schock, G., Miquel, A., 1987. Mass transfer and pressure loss in spiral-wound modules. *Desalination* 64, 339–352.
- Speth, T.F., Summers, R.S., Guess, A.M., 1998. Nanofiltration foulants from a treated surface water. *Environ. Sci. Technol.* 32, 3612–3617.
- Sutherland, I.W., 1999. Polysaccharases for microbial exopolysaccharides. *Carbohydr. Polym.* 38, 319–328.
- Van der Kooij, D., Vrouwenvelder, H.R., Veenendaal, H.R., 2003. Elucidation and control of biofilm formation processes in water treatment and distribution using the unified biofilm approach. *Wat. Sci. Technol.* 47, 83–90.
- Vecchia, E.D., Luna, M., Sethi, R., 2009. Transport in porous media of highly concentrated iron micro- and nanoparticles in the presence of Xanthan gum. *Environ. Sci. Technol.* 43, 8942–8947.

- Vrouwenvelder, H.R., Van Paassen, J.A.M., Folmer, H.C., Hofman, J.A.M.H., Nederlof, M.M., Van der Kooij, D., 1998. Biofouling of membranes for drinking water production. *Desalination* 118, 157–166.
- Vrouwenvelder, J.S., Van Paassen, J.A.M., Wessels, L.P., Van Dam, A.F., Bakker, S.M., 2006. The membrane fouling simulator: a practical tool for fouling prediction and control. *J. Mem. Sci.* 281, 316–324.
- Vrouwenvelder, J.S., Manolarakis, S.A., van der Hoek, J.P., van Paassen, J.A.M., van der Meer, W.G.J., van Agtmaal, J.M.C., Prummel, H.D.M., Kruithof, J.C., van Loosdrecht, M.C.M., 2008. Quantitative biofouling diagnosis in full scale nanofiltration and reverse osmosis installations. *Water Res.* 42, 4856–4868.
- Vrouwenvelder, H.R., Paassen, J.A.M., Kruithof, J.C., van Loosdrecht, M.C.M., 2009a. Sensitive pressure drop measurements of individual lead membrane elements for accurate early biofouling detection. *J. Mem. Sci.* 338, 92–99.
- Vrouwenvelder, H.R., Graf von der Schulenburg, D.A., Kruithof, J.C., Johns, M.L., van Loosdrecht, M.C.M., 2009b. Biofouling of spiral-wound nanofiltration and reverse osmosis membranes: a feed spacer problem. *Water Res.* 43, 583–594.
- Wuertz, S., Spaeth, R., Hinderberger, A., Griebel, T., Flemming, H.-C., Wilderer, P.A., 2001. A new method for extraction of extracellular polymeric substances from biofilms and activated sludge suitable for direct quantification of sorbed metals. *Wat. Sci. Technol.* 43, 25–31.